1ST International Symposium on Nanotechnology
Advance Research Materials Center
Islamic Azad University of Najafabad Branch
11, 12 May, Isfahan Iran

PREPARATION OF MECHANICALLY COMPETENT, BIOACTIVE, AND BIORESORBABLE NANOCOMPOSITE FOAMS FOR BIOMEDICAL APPLICATIONS

Hamed Ghomi

Young Researchers and Elite Club, Najafabad Branch, Islamic Azad University, Najafabad, Iran

Abstract

This work successfully synthesized highly porous, mechanically competent, bioactive, and bioresorbable nanocomposite foams on addition of bioactive glass (BG) to pure hydroxyapatite (HA). Nanocomposite foams were prepared on addition of 63S BG to pure HA, in proportion of 0, 25, 50, 75, and 100 wt.%, and their mechanical properties and bioactivity were compared. The results showed that the nanocomposite foams have a grain size in the range 24-38 nm and pore size in the range 100-400 µm. The compressive strength measurements showed that the compressive strength and elastic modulus increased with increasing the amount of BG addition up to 25 wt.% and then decreased by more addition of BG. In comparison to results of other researchers, the foams compressive strength has increased with decreasing the particle size to nano scale and production of BG reinforced HA. The maximum values of compressive strength and elastic modulus of prepared foams were found to be about 2.78 MPa and 219 MPa, respectively. The mean values of true (total) and apparent (interconnected) porosity were calculated in the range 84-88% and 57-76%, respectively. The high specific surface area of the prepared foams (40.65 $m^2.g^{-1}$), due to the high porosity level (84-88%) and nanosized structure (24-38 nm), increases the rate of bioresorbability and accelerates the deposition process of bone-like apatite, which aids bone repair and fixation. In vitro tests showed that by increasing the amount of BG, the bioactivity and amount of bone-like apatite formed in dependence of immersion time in SBF increased and more pores were filled. The obtained composite foams have chemical composition similar to the mineral phase of bone and by changing the ratio of HA/BG it can reach the appropriate bioactivity and biodegradability level needed for different biomedical applications.

Keywords: *Nanocomposite, Foams, Bioactive glass, Hydroxyapatite, Gelcasting*

1. Introduction

The new challenge in biomaterials is to enhance the body's own regenerative capacity by stimulating genes that initiate repair at the site of damage or disease. A third generation of biomaterials is being developed to do this. The separate concepts of bioactive and biodegradable materials have been combined to make bioactive materials resorbable. Third generation bioactive glasses and macroporous foams are being designed to activate genes that stimulate regeneration of living tissues [1].

Highly porous bioceramic scaffolds (foams) supply a framework for enhanced cell infiltration and migration throughout the scaffold [2], and act as a template for bone growth in three dimensions [3]. Cell spreading and proliferation with bone progenitors were capable of filling 400 µm pores within two weeks [2].

There are many criteria for an ideal tissue-engineering scaffold. Firstly the material used should be biocompatible (not toxic) and promotes cell adhesion and activity (differentiation and proliferation), stimulating new bone growth (osteogenesis). The material should bond to the host tissue without the formation of non-adherent scar tissue. The scaffold should resorbs at the same rate as tissue is repaired, producing degradation products that are non-toxic and stimulate genes in the regenerating tissue to promote efficient cell differentiation and proliferation or can be excreted easily by the body, for example through the respiratory or urinary systems. The structure of the

Corresponding author. Tel.: +98 910 3141226
E-mail address: hamed1985.gh@gmail.com

scaffold should consist of a highly interconnected porous network with porosity ≥ 90%. Interconnections greater than 50 μm in diameter [4] and pores larger than 100 μm in diameter [5] should allow for cell penetration, tissue ingrowth, vascularization and nutrient delivery to the regenerating tissue and assure mineralized bone formation. The mechanical properties of the scaffold should be sufficient to provide mechanical stability in load bearing sites prior to regeneration of new tissue. The processing technique employed to produce the scaffold should allow for the fabrication of irregular shapes, to match those of defect sites, and should possess the potential to produce scaffolds to the required international standards for clinical use [1, 3, 6].

Bioactive ceramics, such as bioactive glasses and hydroxyapatite (HA) have been developed over the last two decades. Their accomplishments in the field of biomedical applications have attracted wide attention [7].

HA is characterized by its high biocompatibility and its close chemical similarity to biological apatite present in hard human tissues [8-10]. The advantage of using HA as a bioceramic or biomaterial compared to other bioceramics, such as bioactive glasses or glass ceramic, is its chemical similarity to the inorganic component of bone and tooth. However, although HA is bioactive, its reactivity with existing bone, and the rate at which bone apposes and integrates with HA, in comparison with bioactive glasses and ceramics, is relatively low [11].

Bioactive glasses are more reactive, degradable, osteoconductive, and show better bioactivity than HA [8-10, 12-14], and have been studied for more than thirty years since Hench first invented Bioglass [15]. Recent studies showed that the degradation products of bioactive glasses could stimulate the production of growth factors, cell proliferation and activate the gene expression of osteoblast [16, 17]. In addition, bioactive glass is the only one, which could bond in a few hours to hard and soft tissue [18, 19].The limiting factor in the use of bioactive glasses as tissue engineering scaffolds is the inherent brittleness of glass [1]

If HA and bioactive glass (BG) are to be combined in an optimized tissue engineering scaffold, then the designed composite offers an exceptional opportunity. The designed composite allows for the creation of bioresorbable and bioactive scaffolds with tailored physical and mechanical properties, and similar chemical composition to biological apatite present in hard human tissues. Moreover, the designed composite can be engineered in such a way that their resorption rate in the body matches the formation rate of new tissue.

Recent studies showed that increasing specific surface area and pore volume of bioactive glasses might greatly accelerate the deposition process of HA [4].Webster et al. revealed that the biomaterials in nanoscale could stimulate the reaction between materials and cells [20, 21]. It was demonstrated by in vitro tests of nano bioceramics (such as HA) that osteoblast proliferation and long term functions could be enhanced when the sizes of bioceramics grains or fibers were less than 100 nm. Furthermore, nanomaterial was one of the components of natural bones, so nanomaterials have been paid much attention in bionics and bone tissue engineering field [22].

The aim of this work was fabrication, in vitro characterization, and optimizing the compressive strength of nanostructure bioceramic composite foams consisting of HA and BG. For this purpose, HA and BG nanopowders were synthesized by the sol-gel method and porous body of HA/BG composite was fabricated by the gelcasting technique.

2. Materials and Methods

2.1. Starting materials

In this study tetraethyl orthosilicate (TEOS, Merck), triethyl phosphate (TEP, Aldrich), calcium nitrate tetrahydrate ($Ca(NO_3)_2 \cdot 4H_2O$, Merck), phosphoric pentoxide (P_2O_5, Merck), absolute ethanol (C_2H_5OH, Merck), and hydrochloric acid (HCl, Merck) were used as HA and BG precursors. In addition to, agarose powder (Merck) as a gelling agent, Tergitol (Aldrich) as a surfactant, and tripoly phosphate sodium (TPP) as a dispersant were used as gelcasting method components.

2.2. Preparation of HA/BG composite foams

HA and BG nanopowders were synthesized by the sol-gel method and different powder compositions were prepared on addition of BG nanopowder to pure HA, in proportion of 0, 25, 50, 75, and 100 wt.% by ball milling (B/P: 5/1, rotational speed: 175 rpm, and time: 45 min). The prepared powders by means of 1 wt.% tripoly phosphate sodium as a dispersant were disperse in deionized water. Simultaneously 7 wt.% Agarose powder as a gelling agent was dissolved in deionized water under stirring using a magnetic stirrer and heating up to 130°C. The agarose solution was added to the stirring slurry of powder at 80°C. The prepared slurry was foamed by vigorous agitation using a triple-blade mixer at 80°C with the addition of 3 vol.% of surfactant. The surfactant used was Tergitol that stabilizes the bubbles that are formed by vigorous agitation. The foamed slurry was then poured into the mold and the gelling reaction (gelation) was catalyzed by cooling the foam to 0°C. The gelation process provides permanent stabilization for the bubbles. The samples were then de-molded, dried at room condition, and thermally stabilized at 900°C for 4 hr. The foams with 50 wt.% BG were sintered at different temperatures to evaluate the effect of sintering temperature.

2.3. Materials characterization

In order to analyze the phase structure of the prepared powders and composite foams, X-ray diffraction (XRD, Philips Xpert) analysis was performed.

Scanning electron microscopy (SEM) evaluations were performed using a Philips XL 30 to investigate the morphology and size of the pores before and after immersing the composite foams in the SBF. The specimens were coated with a film of Au before observation in SEM using sputtering technique. The components of the composite foams were characterized by an energy dispersive spectrometer (EDS) utilizing ZAF corrections.

Transmission electron microscopy (TEM, Philips CM-120) was used to study the morphology and particle size of the prepared powders and the grain size of the prepared foams. The specific surface area of the composite foam with 25 wt.% BG was calculated from the N_2 adsorption isotherms using the multipoint Brunauer-Emmett-Teller (BET) technique.

To determine the porosity of the composite foams, three samples of the foams were selected for each sintering temperature and composition and the porosity of the bulk specimens was measured by Archimedes method.

For measuring the compressive strength of the porous samples a crosshead speed of 0.5 mm/min was used and the compressive tests were performed on samples consisting of cylindrical bars (10 mm in diameter and 20 mm in length) using a universal testing machine. The compressive strength was estimated from the maximum load registered during the test divided by the original area. The results were based on an average of five specimens.

To evaluate the bioactivity and bioresorbability of the prepared foams, the standard SBF was prepared according to Kokubo's protocol and the samples were immersed in the prepared solution. Each prepared specimen was placed in one sterilized polyethylene bottle and SBF with a solid/liquid ratio of 10 mg/ml was added to these bottles. The bottles were hold in a water bath at 36.5± 0.5 °C for various immersion times (7, 14, 21, and 28 days) without refreshing the soaking medium. The specimens were then removed from the solutions, rinsed with deionized water, and dried at room condition. During this time (28 days), the changes in pH value of the solutions were evaluated by a pH meter. The concentration of the calcium and phosphorous ions in the filtered solutions were determined by inductive coupled plasma optical emission spectroscopy (ICP-OES, Perkin Elmer 7300 DV). The bone-like apatite formation on the surface of the samples and pores filling by formation of apatite because of precipitation process of calcium phosphate were investigated by SEM micrographs.

The Fourier transform infrared spectroscopy (FTIR) in the range of 400-4000 cm-1 was utilized to confirm the formation of apatite layer on the samples.

3. Results and discussion

The XRD patterns of the starting HA and BG nanopowders, composite foams with 50 wt.% BG at different sintering temperatures, and foams with 100 and 0 wt.% BG sintered at 900°C are shown in Fig. 1. Good agreement was found between the XRD patterns of the prepared HA powder (Fig. 1c) and the stoichiometric HA. However, the XRD pattern of the HA foam (foam with 0 wt.% BG) sintered at 900°C showed the partial decomposition of HA to beta tricalcium phosphate (β-TCP) phase. The spectra of the foam with 100 wt.% BG sintered at 900°C (Fig. 1b) showed the peaks that were indicative of Larnite (Ca_2SiO_4). It could be noticed that after heat treatment at 900°C, the crystallinity of BG have been increased. This is due to the formation of crystalline phase (Larnite) at approximately 900°C. Crystallization of the BG will affect its bioactivity and resorbability [23]. However, the BG reinforced HA composite foam sintered at 900°C contained a HA phase and variable amounts of β-TCP and amorphous phases, depending on the amount of BG added and did not has any peaks of Ca_2SiO_4. Fig. 1(e-g) show XRD spectra for composite foams with 50 wt.% BG sintered at 700, 800, and 900°C. Spectra of foams sintered at 700 and 800°C showed there were no phase transformations detected when the sintering temperature was less than 900°C. However, when the sintering temperature was as high as 900°C, the X-ray analyses showed the presence of β-TCP phase, which indicates the decomposition of HA and BG. The presence of β-TCP is very important, because it is very soluble phase [24], which favors the scaffolds resorption. By increasing the sintering temperature, the XRD patterns of the composite foams exhibited an increase in peak height and a decrease in peak width, thus indicating an increase in crystallinity and crystallite size. The crystallite size of the composite foams with 50 wt.% BG at different sintering temperatures was estimated by broadening of XRD peaks using Scherrer's formula in the range 24-38 nm.

Fig. 2 shows SEM micrographs of the composite foams sintered at 900°C for 4 hr. SEM micrographs provided information about pore size distribution, morphology and interconnectivity of the pores. SEM micrographs showed that the porous bioceramic structure obtained, consisted of a highly interconnected spherical porous network with the pore size between 100-400 µm. Such analysis of the bioceramic scaffold or foam is important, because it is related to osteoconductive, resorbability, permeability, and mechanical properties. Interconnected and open pores are very

important to allow the flow of substances. For tissue engineering applications, the most important parameter of the porous network is diameter of the interconnecting pore apertures. The interconnected pore diameter should be greater than 100 µm to be suitable for tissue engineering applications and allow tissue ingrowth and finally vascularization [25].

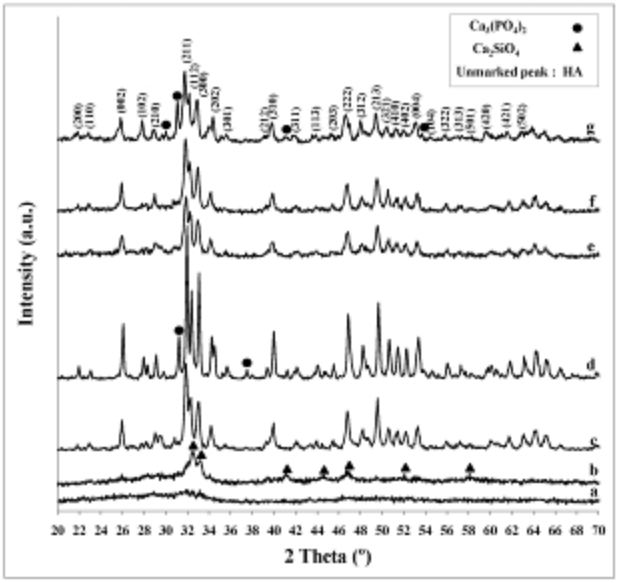

Fig. 1 XRD patterns of the prepared (a) BG nanopowder, (b) foam with 100 wt.% BG sintered at 900°C for 4 hr, (C) HA nanopowder, (d) foam with 0 wt.% BG sintered at 900°C for 4 hr, and (e-g) composite foams with 50 wt.% BG sintered at 700, 800, and 900°C for 4 hr, respectively.

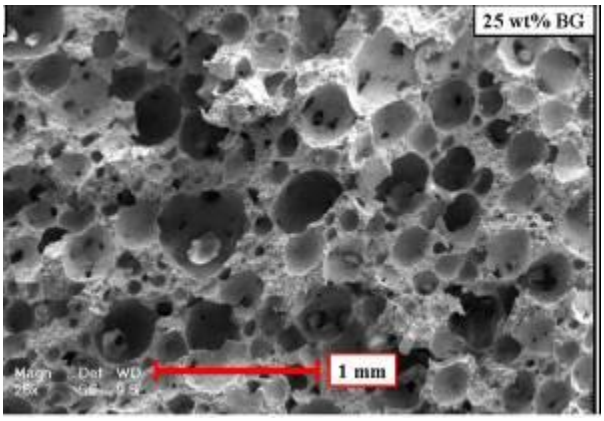

Fig. 2 SEM micrographs of the composite foams sintered at 900°C for 4 hr.

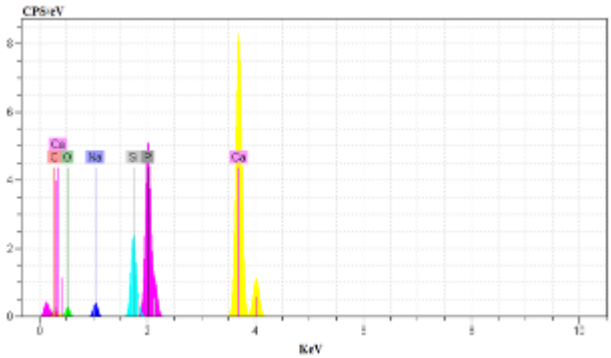

Fig. 3 EDS spectrum of the composite foam with 25 wt.% BG sintered at 900°C for 4 hr.

Table 1: True and apparent porosity, compressive strength, and elastic modulus of the nanocomposite foams with different compositions at different sintering temperatures

Composition	Sintering temperature	True porosity	Apparent porosity	Compressive strength (MPa)	Elastic modulus (MPa)
0 wt.% BG	900 °C	84 (± 1)	57 (± 2)	1.36 (± 0.09)	146 (± 15)
25 wt.% BG	900 °C	85 (± 1)	59 (± 1.5)	2.78 (± 0.11)	219 (± 9)
50 wt.% BG	900 °C	86 (± 1.5)	60 (± 2)	1.95 (± 0.16)	204 (± 6)
75 wt.% BG	900 °C	86 (± 2)	66 (± 1)	1.21 (± 0.05)	78 (± 7)
100 wt.% BG	900 °C	88 (± 2)	76 (± 2)	0.92 (± 0.09)	57 (± 11)
50 wt.% BG	800 °C	88 (± 1)	67 (± 1.4)	1.54 (± 0.08)	148 (± 12)
50 wt.% BG	700 °C	91(± 1.7)	71 (± 1.8)	0.87 (± 0.12)	92 (± 5)

Fig. 3 shows EDS spectra of the foam with 25 wt.% BG. As shown in Fig. 3, the existence of phosphorus, calcium, oxygen, carbon, and silicon are related to hydroxylcarbonate apatite (HCA) and BG.

Table 1 summarizes the true and apparent porosity, compressive strength, and elastic modulus of the nanocomposite foams as a function of foams composition and sintering temperature.

The mean values of true and apparent porosity for the composite foams with 50 wt.% BG at different sintering temperatures were calculated in the range 86-91% and 60-71%, respectively. The maximum values are related to minimum sintering temperature. Furthermore, the mean values of true and apparent porosity for the composite foams with different compositions, which were sintered at 900°C for 4 hr, were measured in the range 88-84% and 57-76%, respectively.

The mean values of compressive strength and elastic modulus for the composite foams with different compositions, which were sintered at 900°C, were measured in the range 0.92-2.78 MPa and 57-219 MPa. In fact, sintering at 900°C for 4 hr provides an optimal combination of compressive strength together with the macroscopic structural features appropriate for bone ingrowth and angiogenesis. The foams with compressive strength of 2.78MPa were fabricated while maintaining interconnected pore size in excess of 100 µm. The compressive strength of the composite foams increased with increasing the amount of BG to 25 wt.%, and more addition of BG leads to decrease the two mechanical properties mentioned above. Also, in order to determine the effect of sintering temperature on the mentioned mechanical properties the compressive tests were performed on composite foams with 50wt.% BG, at different sintering temperatures (700, 800, and 900°C for 4 hr) and the mean values of compressive strength and elastic modulus were measured in the range 0.87-1.95 MPa and 92-204 MPa. It showed that the compressive strength of the foams increased with increasing the sintering temperature due to less porosity and pore size, which was in good agreement with other reports [26].The compressive strength of the composite foams with 25wt.% BG, after sintering at 900°C for 4 hr was achieved to 2.78 MPa, which is close to the standard for a porous bioceramic bone implant (2.4 MPa) and within the lower limit of the compressive strength of trabecular bone (2-12 MPa) [27]. The obtained compressive strength in comparison to compressive strength results of other researchers for bioceramic foams with different compositions [28-30], demonstrates the foams compressive strength has increased with decreasing the particle size and production of BG reinforced HA. Moreover, decreasing particle size through increasing the specific surface area facing with body fluid, improved osteoblast functions are proliferation, alkaline phosphatase synthesis, and calcium containing mineral deposition [20, 22].

Fig. 4 shows TEM micrographs of the sintered foams at 900°C with 50 wt.% BG. TEM micrographs illustrate the grain size to be smaller than 50 nm.

The BET specific surface area obtained from BET plot was found to be 40.65 $m^2.g^{-1}$.

The in vitro studies were successful in confirming the high ability for apatite formation on the surface of the composite foams, which is a measure of the considerable bioactivity of the material. Fig. 5 shows SEM micrographs of composite foams with different compositions after 28 days of immersion in SBF. It is apparent that the bone-like apatite on the surface and inner wall of pores are formed as a result of contact of these composite foams with SBF. The functional groups of the white particles nucleated on the surface of the foams were investigated using FTIR. The foam with 100 wt.% BG was selected because it was completely free of HA, so the formation of HA because of soaking in SBF could be indicated clearly. FTIR confirmed that apatite formation took place on the foams surface after immersion in SBF and the white particles are bone-like apatite.

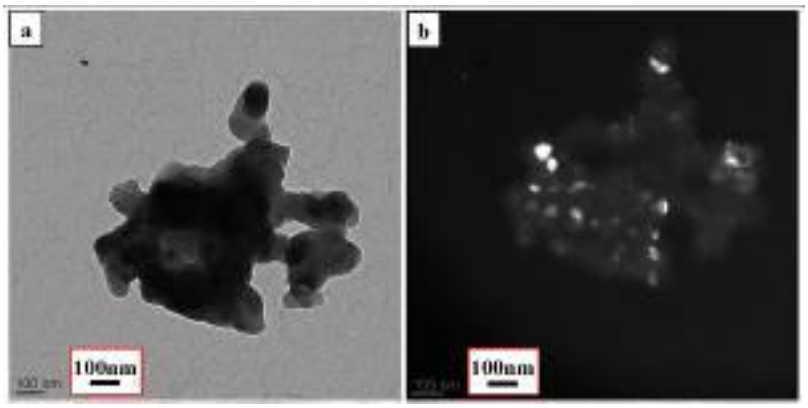

Fig. 4 TEM micrographs of the composite foam with 50 wt.% BG sintered at 900°C for 4 hr.

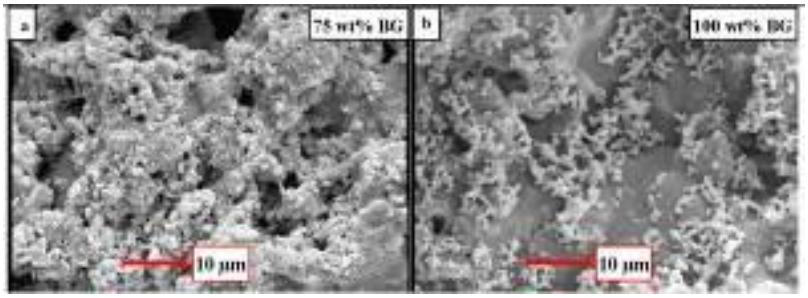

Fig. 5 SEM micrographs of the composite foams with different compositions after 28 days of immersion in SBF.

Fig.6 shows the effect of foams composition on the Ca and P ion concentrations, at different soaking times. SBF contains approximately 80 ppm of calcium ions. The release profiles of calcium from composite foams sintered at 900°C show that the calcium ion concentration increases by increasing the soaking time and the amount of BG. Increasing of calcium ion concentration by increasing the soaking time, implying high bioactivity and resorbability of BG. It shows that the rate of BG dissolution is more than the rate of calcium ions deposited on the foams surface. Increasing of calcium ion concentration by increasing the amount of BG is related to more bioactivity and resorbability of BG in comparison to HA. SBF contains 30 ppm of phosphorous ions. The release profiles of phosphorous from composite foams sintered at 900°C show that there is a decrease in concentration of phosphorous in SBF by increasing the soaking time due to formation of the HCA layer on the foams surface and slowly dissolution of phosphorus from the foams in SBF as reported by other researchers [31, 32].

Furthermore, decreasing of phosphorous by increasing the amount of BG shows the enhanced ability of formation of the HCA layer.

Furthermore, in order to determine the effect of sintering temperature, the dissolution profiles and graphs of the pH trends for the composite foams with 50wt.% BG as a function of soaking time, for each sintering temperature are shown in Fig. 7.

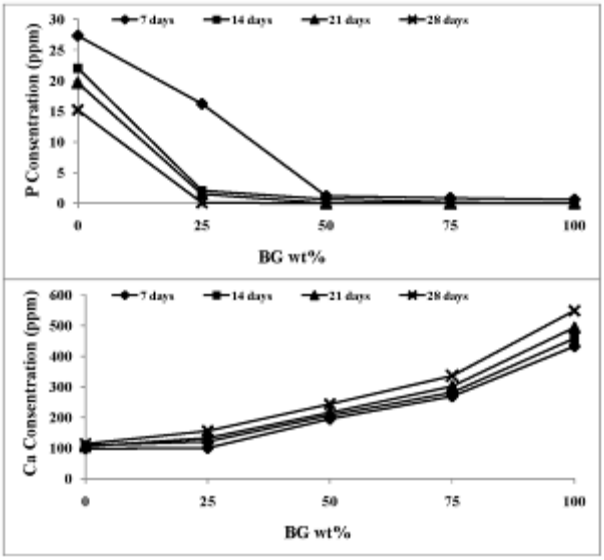

Fig. 6 Effect of the foams composition on Ca and P ion concentrations at different soaking times.

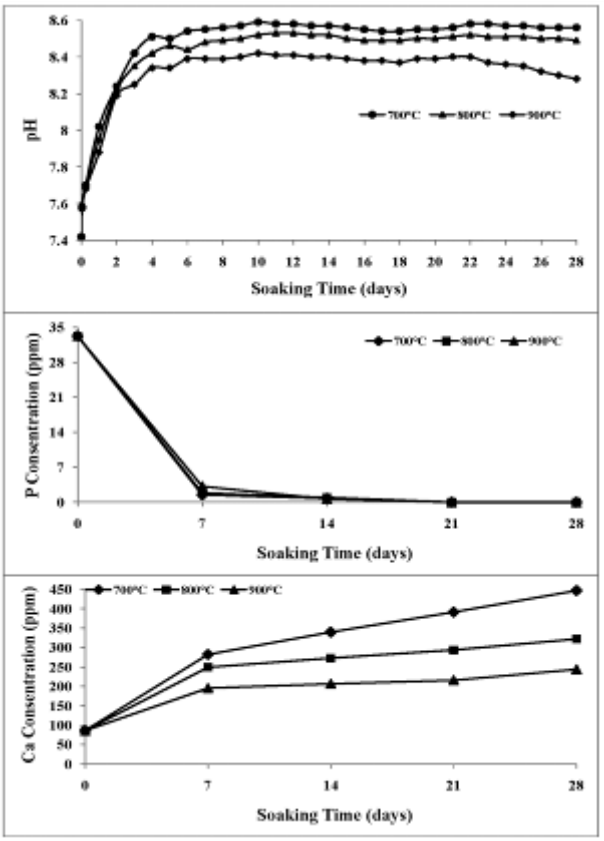

Fig. 7 The dissolution profiles and graphs of the pH trends for the composite foams with 50wt.% BG as a function of soaking time for each sintering temperature.

Fig. 7 shows the pH value and the amount of calcium and phosphorous released from foams generally decreased as sintering temperature was increased from 700 to 900°C. This is due to increasing the crystallinity and crystallite size by increasing the sintering temperature. This is in agreement with the results of other research [31].

4. Conclusions

Nanocomposite foams on addition of 63S BG with 65% SiO2, 31% CaO, and 4% P2O5 (in mol%) to pure HA, in proportion of 0, 25, 50, 75, and 100wt.% were successfully fabricated and their mechanical properties and bioactivity were compared. The results showed that the nanocomposite foams have a particle size in the range 20-42 nm and pore size in the range 100-400 μm. The compressive strength measurements showed that the compressive strength and elastic modulus increased with the increasing amount of BG addition up to 25wt.% and then decreased by more addition of BG. The maximum values of compressive strength and elastic modulus were found to be about 2.78MPa and 219MPa, respectively, which are close to the lower limit of the compressive strength and elastic modulus of cancellous bone. The compressive strength is close to the standard for a porous bioceramic bone implant (2.4MPa). The mean values of the true and apparent porosity were calculated in the range 88-84% and 57-76%, respectively. In vitro tests showed that by increasing the amount of BG, the bioactivity and amount of bone-like apatite formed in dependence of immersion time in SBF increased and more pores were filled. The resulting composite foams have similar chemical composition to the mineral phase of bone and by changing the ratio of HA/BG can reach the appropriate bioactivity and biodegradability level needed for different applications. Considering the results obtained, it seems that, manufactured foams could be a good candidate for tissue engineering applications such as drug delivery and cell loading, but cell culture and in vivo tests are needed for more assurance.

References

1- Shirtliff V.J, Hench L.L. Bioactive materials for tissue engineering, regeneration and repair. J. Mater. Sci. 2003; 38(23): 4697-707.

2- Oh S, Oh N, Appleford M, L. Ong J. Bioceramics for Tissue Engineering Applications. Am. J. Biochem. Biotechnol. 2006; 2: 49-56.

3- Jones J.R, Lee P.D, Hench L.L. Hierarchical porous materials for tissue engineering. Philosophical Transactions of the Royal Society. A-Mathematical Physical and Engineering Science 2006; 364: 263-81.

4- Lu J.X, Flautre B, Anselme K, Hardouin, Gallur A, Descamps M, et al. Role of interconnections in porous bioceramics on bone recolonization in vitro and in vivo. J. Mater. Sci. Mater. Med. 1999; 10: 111-20.

5- Freyman T.M, Yannas I.V, Gibson L. Cellular materials as porous scaffolds for tissue engineering. J. Prog. Mater. Sci. 2001; 46: 273-82.

6- Darmawati M.y, Oana B, Aldo R.B. Polymer-bioceramic composite for tissue engineering scaffolds. J. Mater. Sci. 2008; 43: 4433-42.

7- Liu D.M, Chou H.M. Formation of a new bioactive glass ceramic. J. Mater. Sci. Mater. Med. 1994; 5: 7-10.

8- Hench L.L, West J.K. Biological applications of bioactive glass. Life Chem. Rep. 1996; 13:187-241.

9- Vallet-Reg M. Ceramics for medical applications. J Chem Soc, Dalton trans 2001; 97-108.

10- Oonishi H, Hench L.L, Wilson J, Sugihara F, Tsuji E, Matsuura M, et al. Quantitative comparison of bone growth behaviour in granules of Bioglass, A-W glass ceramic, and hydroxyapatite. J. Biomed. Mater. Res. 2000; 51:37-46.

11- Tang X.L, Xiao X.F, Liu R.F. Structural characterization of silicon substituted hydroxyapatite synthesized by a hydrothermal method, Mater. Lett. 2005; 59 :3841-46.

12- Hench L.L. The challenge of orthopaedic materials, Curr. Orthop. 2000; 14: 7-15.

13- Wilson J, Low S.B. Bioactive ceramics for periodontal treatment: comparative studies in the Patus monkey.J. Appl. Biomater. 1992; 3: 123-9.

14- Vallet-Regi M, Ragel C.V, Salinas A. Glasses with Medical Applications J. Eur. J. Inorg. Chem. 2003: 1029-42.

15- Hench L.L, Splinter R.J, Allen W.C, Greenlee T.K. Bonding mechanisms at the interface of ceramic prosthetic materials J. Biomed. Mater. Res. 1971; 5: 117-41.

16- Lossdorfer S, Schwartz Z, Lohmann C.H, Greenspan D.C, Ranly D.M, Boyan B.D. Osteoblast response to bioactive glasses in vitro correlates with inorganic phosphate content. Biomater. 2004; 25(13): 2547-55.

17- Valerio P, Pereira M.M, Goes A.M, Leite M.F. The effect of ionic products from bioactive glass dissolution on osteoblast proliferation and collagen production. Biomater. 2004; 25(15): 2941-8

18- Hench L.L, Xynos I.D, Polak J.M. Bioactive glasses for in situ tissue regeneration. J Biomater. Sci. Polym. Ed. 2004; 15: 543-62.

19- Sehrooten J, Helsen J.A. Adhesion of bioactive glass coating to Ti6Al4V oral implant. Biomater. 2000; 21: 1461-69.

20- Webster T.J, Ergun C, Doremus R. H, Siegel R.W, Bizios R. Specific proteins mediate enhanced osteoblast adhesion on nanophase ceramics. J. Biomed. Mater. Res. 2000; 5: 475-83.

21- Webster T.J, Siegel R.W, Bizios R. Osteoblast adhesion on nanophase ceramics, Biomater. 1999; 20: 1221-27.

22- Webster T.J, Ergun C, Doremus R.H, Siegel R.W, Bizios R. Enhanced functions of osteoblasts on nanophase ceramics. Biomater. 2000; 21: 1803-10.

23- Atwood R.C, Jones J.R, Lee P.D. L.L. Hench Analysis of pore interconnectivity in bioactive glass foams using X-ray microtomography. Scripta Materialia 2004; 51: 1029-33.

24- Hench LL. Bioceramics. J. Am. Ceram. Soc. 1998; 81(7): 1705-28.

25- Hench LL, Xynos ID, Edgar AJ, Buttery LDK, Polak JM. Gene activating glasses. Int. congress on glass 2001; 1: 226-33.

26- Jones JR, Ehrenfried LM, Hench LL. Optimising the strength of macroporous bioactive glass scaffolds. Key Eng. Mater. 2004; 254-6: 981-4.

27- Carter DR, Hayes WC. Bone compressive strength: the influence of density and strain rate. Science 1976; 194: 1174-6.

28- Potoczek M. Hydroxyapatite foams produced by gelcasting using agarose. Mater. Lett. 2008; 62(6-7): 1055-7.

29- Potoczek M, Zima A, Paszkiewicz Z, Slosarczyk A. Manufacturing of highly porous calcium phosphate bioceramics via gel-casting using agarose. Ceram. Int. 2009; 35: 2249-54.

30- Sepulveda P, Ortega F.S, Innocentini M.D.M, Pandolfelli V. C. Properties of highly porous hydroxyapatite obtained by the gelcasting of foams. J. Am. Ceram. Soc. 2000; 83(12): 3021-24.

31- Jones J.R, Ehrenfried L.M, Hench L.L. Optimising bioactive glass scaffolds for bone tissue engineering. Biomater. 2006; 27: 964-73

32- Hench L.L, Jones J.R, Sepulveda P. Bioactive materials for tissue engineering scaffolds, ln:Future Strategies for Tissue and Organ Replacement, Editor(s): Polak, Hench, Kemp, London, Imperial College Press, 2002: 3-24.